

Ask the plants directly: Understanding plant needs using electrical impedance measurements

Original

Ask the plants directly: Understanding plant needs using electrical impedance measurements / Garlando, Umberto; Calvo, Stefano; Barezzi, Mattia; Sanginario, Alessandro; Motto Ros, Paolo; Demarchi, Danilo. - In: COMPUTERS AND ELECTRONICS IN AGRICULTURE. - ISSN 0168-1699. - 193:(2022), p. 106707. [10.1016/j.compag.2022.106707]

Availability:

This version is available at: 11583/2954292 since: 2022-01-31T20:36:36Z

Publisher:

Elsevier

Published

DOI:10.1016/j.compag.2022.106707

Terms of use:

This article is made available under terms and conditions as specified in the corresponding bibliographic description in the repository

Publisher copyright

Elsevier postprint/Author's Accepted Manuscript

© 2022. This manuscript version is made available under the CC-BY-NC-ND 4.0 license
<http://creativecommons.org/licenses/by-nc-nd/4.0/>. The final authenticated version is available online at:
<http://dx.doi.org/10.1016/j.compag.2022.106707>

(Article begins on next page)

18 achieved with a system designed by the authors and validated by showing relations (correla-
19 tion and Granger's causality) between stem electrical impedance and environment parameters.
20 Validation was accomplished by monitoring and analyzing multiple plants at the same time. Sta-
21 tistical analysis showed a correlation of up to 95% between impedance and soil moisture, and
22 that soil moisture variations caused variation in the impedance of the plants.

23 **Keywords**— Impedance measurements, in-vivo, sensor system, plant health

24 **1 Introduction**

25 The world's population is growing, and it is expected to reach over 10 billion this century, as stated by UN.
26 Population Division (2019). Furthermore, arable lands on the planet are decreasing. Although this is mainly
27 due to urbanization in some regions (such as northern Europe), this is not the case for warmer climate territo-
28 ries. As stated by the European Environment Agency (2020), by Burrell et al. (2020), and by Mahato (2014),
29 the reduction of arable lands is primarily due to both climate change and land usage. Arable land reduc-
30 tion and world population growth are the two main factors causing the problem of food security. Producing
31 enough food to feed the entire world population is becoming critical, and new approaches are needed to face
32 this issue.

33 Smart agriculture can improve food production and, therefore, food security. Sensors and electronics are
34 used to monitor and intervene in every aspect of the food chain, from crops to final consumers. Integrating
35 sensor data with farmers' experience leads to increased production and reduced waste of resources: mon-
36 itoring climate and crops condition enables the actuation of a precise watering strategy, reducing the use of
37 pesticides (Berenstein and Edan 2017), and increasing crop yield. Currently, environmental parameters are
38 widely inspected, and numerous examples are present in literature (Garlando et al. 2020a). Indirect measure-
39 ment is the most adopted solution nowadays. Custom weather stations are present in literature, like the ones
40 presented by Tenzin et al. (2017) and Kasama et al. (2019). Soil is another important category of parameters

41 widely considered by the research community. Soil moisture, in particular, is a key factor in the wellness of
42 plants. Different approaches to measuring soil moisture are available. Nakayama et al. (2008) inspected soil
43 thermal conductivity and capacity while Daskalakis et al. (2014) detected soil moisture level with a receiving
44 antenna which performed signal frequency modulation.

45 However, measuring environmental conditions is not enough to understand plant status. Therefore, an-
46 other approach is to monitor plant parameters directly. For example, Ramos-Giraldo et al. (2020) measured
47 water stress with a camera pointed at plants and not by inspecting the soil. Similarly, Palazzi et al. (2019)
48 stated that comparing leaf temperature with that of air makes it possible to perform soil moisture measure-
49 ments. Thus the sensor they developed is clipped on a leaf. It measures leaf and air temperature and sends
50 valuable data to the farmer to understand when to irrigate the fields. These examples require expensive and
51 special sensors, making this approach difficult to implement.

52 It has been discovered that valuable information regarding plant status can be derived inspecting plant
53 electrical impedance. Garlando et al. (2020b) discovered that stem electrical impedance rises when the plant
54 dries out and drops after it gets watered. It means that by evaluating in-vivo plant stem impedance over time,
55 it is possible to understand when the plant needs to be watered. Therefore, focusing on electrical impedance
56 measurements could pave the way to developing small, low-cost, smart devices specifically monitoring each
57 plant in the target field. In-vivo plant electrical impedance analysis was also carried by Bar-On et al. (2021).
58 They extracted a lumped element model to mimic the behavior of stem impedance with respect to the injected
59 signal frequency. Their studies have been conducted on *Nicotiana Tabacum* plants. Although it represents
60 a step forward in deepening the knowledge of stem electrical impedance behavior, at the moment, it has
61 not been developed to provide high-level information in real-time. Borges et al. (2012) had also performed
62 *Electrical Impedance Spectroscopy* and Kobata and Honda (2014) exploited *Finite Element Modeling* to solve
63 partial differential equations and infer information about a plant's status. Similarly, Corono-Lopes et al. (2019)
64 applied *Electrical Impedance Tomography* to the volume in proximity of plant roots to achieve pathogen
65 detection. Differently from previous authors, Jinyang et al. (2016) implemented a technique to diagnose

66 potassium stress. The technique relies on impedance spectroscopy of tomato plant leaves carried out in
67 a wide range of frequencies. Analyzing their response with respect to frequency, they extract a model to
68 detect the lack of potassium. Apart from Garlando et al. (2020b) who presented a first approach meant to be
69 expanded further, these latter studies concerned with complex, time-consuming, and not real-time or in-vivo
70 techniques.

71 Our approach was to monitor in-vivo plant stem impedance: impedance variations are then analyzed to
72 assert their relation with external parameters. Our ultimate long-term goal is to remove all the environmental
73 sensors and rely on direct measurement of plant parameters only, eventually placing the sensors directly on
74 the plants themselves and leveraging the stem as the communication channel among them as done by Motto
75 Ros et al. (2019).

76 Our experiments used a bench impedance analyzer and a dedicated sensor node to determine relation-
77 ships among electrical impedance and environmental data. Sensors collected data regarding soil moisture
78 level, air temperature and humidity, and ambient light intensity. At the same time, a multiplexer-based system
79 (described in section 2) analyzed stem electrical impedance of multiple plants simultaneously. The sensor
80 node improved a prototype presented by Bar-on et al. (2019b).

81 The paper is organized as follows. Section 2 describes the measuring system and how measurements
82 were performed. Section 3 shows measurement results and the statistical analysis performed on data. Finally,
83 conclusions are derived in section 4.

84 **2 Materials and Methods**

85 In this section, the different components of the presented system are depicted. The novel measuring system
86 measures both environmental parameters and plants stem impedance. Furthermore, plants used in the
87 experiments are also introduced.

88 **2.1 Impedance measuring system**

89 Impedance measurements were performed using a Keysight 4294A impedance analyzer. It is a bench instru-
90 ment ranging from 40 Hz to 100 MHz used to acquire accurate impedance values in this stage of the analysis.
91 A four-wire measuring system was adopted (Bar-on et al. 2019a) to increase accuracy and reduce error due
92 to interconnections. Implementing the four-wire measuring system was possible thanks to the use of two
93 *Kelvin's* clips per plant and connecting instrument wires as reported by Janesch (2013). Each clip contains
94 two of the four wires needed for this measurement methodology. In these devices, a force-and-sense pair is
95 connected to a single clip (one per jaw). The same instrument was used to monitor multiple plants, thanks to
96 a multiplexing system. Each channel of the impedance analyzer was connected to up to four plants thanks
97 to commercial multiplexers. Multiplexers are based on relays: two relays connect both the signal and ground
98 terminal of two BNCs. In this way, cables coming from the impedance analyzer are alternatively connected
99 to up to four plants. The selected multiplexers have a serial interface that was used to control the relays and
100 change the interconnections. A Raspberry Pi was used to send control commands to the multiplexers. The
101 impedance analyzer was connected to a PC running a LabVIEW program that managed the measurement
102 procedure and stores impedance spectra. The LabVIEW script was synchronized with the multiplexing con-
103 trol in order to sample the plants under test. Small stainless steel needles, 0.4 mm diameter, were inserted
104 into each plant stem, as depicted in Figure 1. Needles were placed at a distance of 5 cm, with the bottom one
105 placed 3 cm above the ground. Kelvin clips were used to connect the electrodes inserted in the plant stems
106 to the instrument. Impedance measurements were triggered every 15 minutes, resulting in a sampling period
107 of one hour for each plant.

108 **2.2 Environment sensing node**

109 A sensor node for the environmental parameters was also developed. It was used to monitor parameters
110 surrounding the plant under test. In particular, the sensor node measured light intensity, ambient temperature,
111 relative humidity, and soil moisture. Other essential soil parameters were not considered to reduce sensor

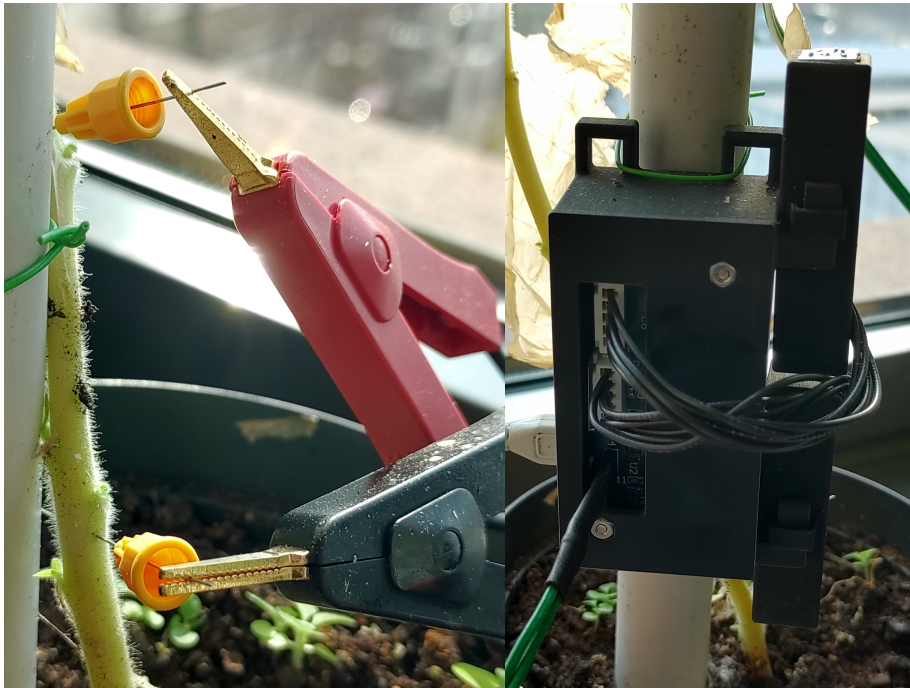


Figure 1: Pictures of the measuring system. Left: detailed view of the needles and kelvin clips used to measure impedance of the stem. Right: sensor case for environmental measurements. The central box contains the Raspberry Pi with the custom designed PCB. The two small boxes connected with the cables hold the temperature, humidity and light sensors. The green cable connects the Watermark sensor.

112 node cost and complexity. Moreover, soil moisture has been considered to be the leading parameter affecting
113 stem impedance. It is probably the most analyzed soil parameter and one of the easiest ones to inspect.
114 Nevertheless, not considering other soil parameters can be a system's limitation since some of them, such as
115 soil salinity or nutrient concentration, may influence stem electrical impedance. A custom PCB to be placed
116 on top of a Raspberry Pi ZERO W was developed. In this way, wireless communication was used to configure
117 the nodes and acquire data. The PCB has two headers for I²C connection to external sensors. Temperature,
118 humidity, and light sensors were mounted on a small PCB connected to the central one. Two integrated
119 circuits were used to monitor those parameters. The former is a Texas Instruments (TI) HDC2080, a digital

120 sensor that embeds an ADC and can sample temperature and relative humidity. It has excellent accuracy
121 and very low power consumption. The latter is a TI OPT3001, an ambient light sensor with automatic range
122 detection and low power capabilities. Short wires were used to connect the two boards to the main system.
123 Furthermore, it is possible to add other sensors in future applications using an empty header already available
124 on the board.

125 A different approach was needed for the soil moisture sensor. An Irrrometer Watermark sensor was used
126 to measure soil water tension. It is a gypsum block, and its resistance changes depending on soil moisture
127 level. The manufacturer provides a curve that relates resistance values to moisture ones. The soil moisture
128 level is provided in kPa since it is derived from soil water potential. This is defined as the amount of energy
129 required for a plant to perform work to extract moisture from the soil, and it is evaluated per unit of volume:
130 thus soil moisture unit of measure turns out to be a pressure. Moisture values extracted by the sensor
131 are negative since it performs differential measurements: the read gypsum's resistance is compared with
132 a reference one assessed in an environment with known humidity conditions. In the sensor's datasheet, it
133 is reported that moisture values below -200kPa must be discarded since they exceed the lowest value this
134 sensor can accurately detect. The main issue with this sensor is that a DC current flowing inside its electrodes
135 could damage the device. Therefore, a pseudo-AC circuit is suggested: a multiplexer rapidly connects and
136 disconnects the sensor terminal to VDD and GND. However, this solution is needlessly complex for our case:
137 it enables connecting multiple sensors to the same system, but only one was used in the actual sensor node.
138 Therefore, another approach was adopted in order to reduce complexity and avoid sensor damage. The
139 schematic of the designed circuitry is depicted in Figure 2.

140 The idea was to use a timer with the watermark sensor in the feedback loop. In this way, the resistance
141 value of the sensor affects the frequency generated by the timer ensuring only AC in the sensor. Furthermore,
142 a power switch, a SiP32432 from Vishay Siliconix, was used to reduce power consumption. When the *Sensor*
143 *On* signal is "low", the power source is disconnected from the timer portion of the circuit. When it is "high",
144 the timer is correctly powered, and it generates a frequency signal that the Raspberry processor can read.

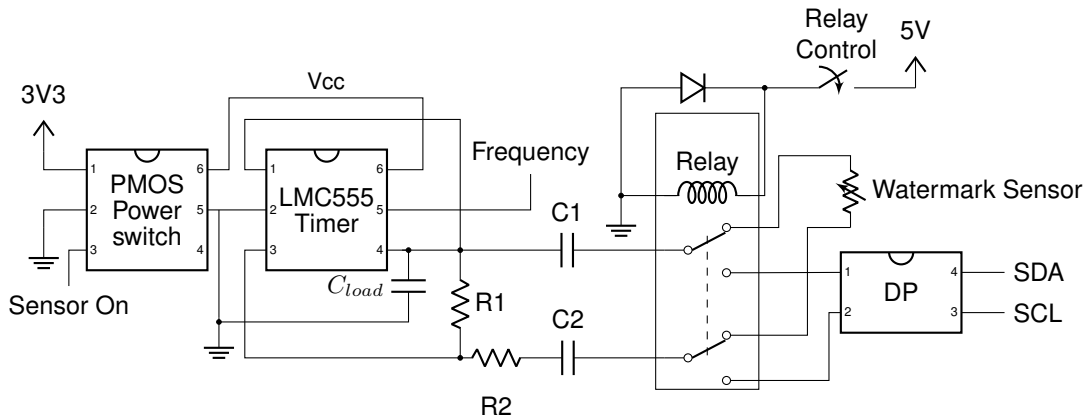


Figure 2: Schematic of the watermark sensor reading circuitry

145 A TI LMC555 timer was used in this case. *Pin 2* and *pin 6* of the timer were used to provide ground and
 146 power supply, respectively. *Pin 3* is the output of the timer: this signal is connected to the load capacitor
 147 C_{load} through the resistive network formed by $R1$, $R2$, and the watermark sensor. These two resistors were
 148 used to set minimum and maximum frequency: when the watermark sensor is disconnected or fully dry, $R1$
 149 limits the current in the load and, therefore setting the minimum frequency. Similarly, when the watermark
 150 sensor is fully wet, and its resistance is almost zero, $R2$ can be considered in parallel with $R1$, thus setting
 151 the maximum frequency. The two capacitors, $C1$ and $C2$, are used to block the DC component flowing in the
 152 sensor in series with the sensor. Threshold (*Pin 1*) and trigger (*Pin 4*) pins are both connected to C_{load} . In
 153 this way, the timer works in direct feedback mode, where its output charges the capacitor, and the same value
 154 is used to trigger the polarity change in the timer. Finally, *Pin 5* is the discharge pin: it is an open collector
 155 output that changes the timer's output pin accordingly. The Raspberry sensed this signal to measure the
 156 generated frequency. Frequency range can be defined by selecting the values of the components. C_{load} was
 157 set to $0.1\mu\text{F}$ while $R1$ and $R2$ to $150\text{k}\Omega$ and 390Ω respectively. A value of $4.7\mu\text{F}$ was selected for both $C1$ and
 158 $C2$. With those values, the generated frequency ranges from about 50Hz to 14.5kHz .

159 A relay was used to disconnect the watermark circuitry when it is not measured. A reed relay with a
 160 nominal coil voltage of 5V was inserted in the circuitry. In this way, it was possible to activate the relay

Stem's Impedance With and Without Relays

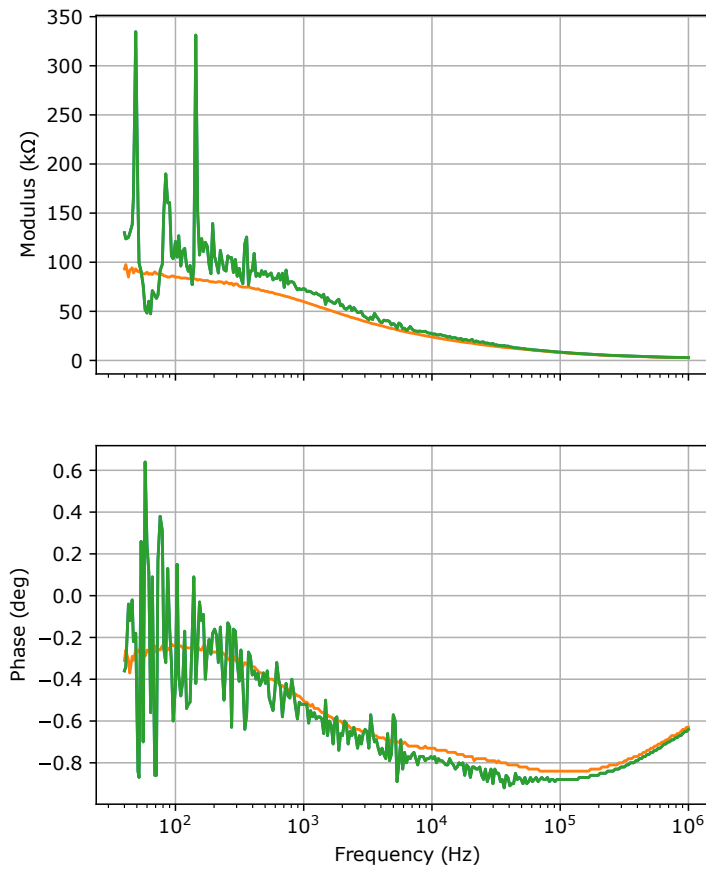


Figure 3: Impedance modulus and phase of the same plant when the watermark sensor is connected to the reading circuitry (green lines) and with the relay used to disconnect it (orange lines). The measurements were taken a few minutes away from each other in order to have similar conditions.

161 with the 5 V pin of the Raspberry Pi and a power switch controlled by an enabling signal. A reed relay was
162 selected instead of a solid-state one to ensure galvanic isolation of the sensor when it is not needed. In
163 this way, any potential noise injected by the reading circuitry is avoided. Furthermore, ground loops can
164 be prevented thanks to this solution. This is not achievable with other kinds of switches. Moreover, an
165 automatic calibration function was implemented. A digital potentiometer, AD5272 by Analog Devices, provides
166 resistance values to the timer circuit. In particular, this potentiometer has a 1% tolerance on the selected
167 resistance value. Therefore it is suitable for a calibration procedure. During the calibration, specific resistive
168 values were selected. The Raspberry set the potentiometer values via I²C communication and read the
169 frequency generated by the timer. Acquired pairs are stored in memory, and when the watermark sensor
170 is measured, the resistance is interpolated from calibration data. The entire procedure can be performed
171 automatically, thanks to the adoption of a double SPDT (Single Pole Double Throw) relay. When it is not
172 powered, the timer circuitry is connected to the potentiometer's wiper terminals. On the contrary, the timer is
173 connected to the sensor when the current flows in the coil.

174 The described circuitry reduced the complexity of the sensor reading procedure: the program running on
175 the Raspberry Pi counts the number of edges in a unit of time, evaluating the frequency. The manufacturer
176 then provides a curve to relate resistance values to water tension (expressed in kPa). The relay adds com-
177 plexity to the circuitry, but it solves other issues, i.e., the calibration curve from frequency to resistance and
178 the direct path to ground when the sensor is inserted in the soil. Components tolerance could slightly modify
179 the relation between sensor resistance and the measured frequency. Manual calibration was possible but not
180 practical: the relay and the digital potentiometer automate the procedure. The other issue was even more
181 severe: with the sensor inserted in the pot and the plant under measurements, a ground loop with the power
182 source of the Raspberry Pi is formed. This last configuration was tested, and Figure 3 shows the obtained
183 results. The design without the relay clearly presents noise in the impedance spectrum.

184 The final PCB was designed to match the Raspberry Pi ZERO W dimensions and stacked directly on top
185 of it. Given the reduced components' cost, each plant is equipped with a dedicated board during the exper-

186 iments. Figure 1 shows the resulting measurement node. Thanks to Raspberry Pi's wireless capability, it is
187 possible to use a central computer to monitor each sensor node. The resulting wireless sensor network could
188 be deployed inside laboratories or greenhouses, where a Wi-Fi network and power sources are available. A
189 Python script with a graphical user interface reads the sensor data and stores them periodically. The script is
190 used to configure time intervals among the measurements and also to perform sensor calibration.

191 **2.3 Plants used in the tests**

192 In the following, plants are numbered from one to five. Each one is a tobacco (*Nicotiana tabacum*) plant
193 growing inside a single pot. This plant species was chosen because of its completely sequenced genome,
194 and since its life-cycle is widely known. Moreover, it could adapt perfectly to climatic conditions present in
195 the laboratory where the analyses were conducted. As described before, each plant was associated with one
196 sensor node. Plants were tested for up to one month. Sometimes periods in which plants were analyzed did
197 not overlap to investigate how plants reacts in different periods of the year. During the experiment, plants were
198 not watered regularly. Water stress conditions were induced in plants, and watering events were performed
199 when their conditions were critical. Plants' conditions criticality was asserted by merging information extracted
200 by sensors and visual analysis (mainly leaves color and stem and leaves turgescence). Moreover, two of the
201 five plants were analyzed during the same period and kept in close proximity. Thus they were exposed to the
202 same environmental conditions, except for soil moisture. One was watered regularly (twice per week), while
203 the other was kept under water stress and watered when its conditions were critical. This has been done
204 as a first step to disentangle each environment parameter's contribution to stem impedance. Each plant was
205 about 50 cm to 60 cm high.

Plant3, Experiment 31 October - 10 November

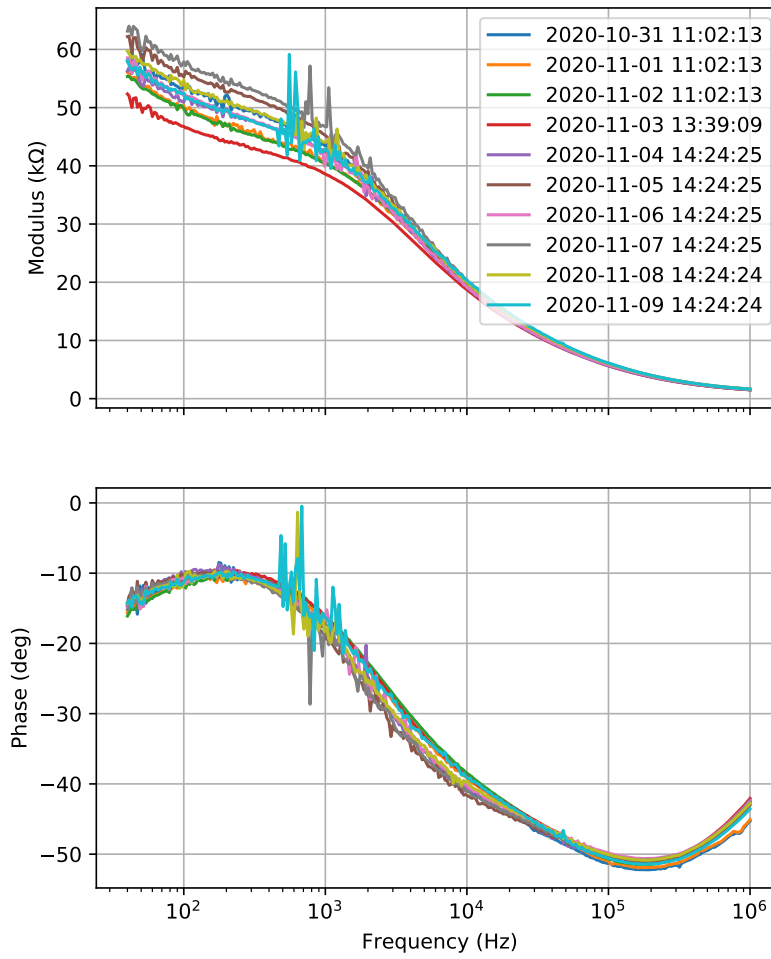


Figure 4: Example of impedance spectrum. Each color represents measurements in different days

3 Results and Discussion

Figure 4 shows the impedance spectrum of a single plant over ten days. Different spectra are superposed to show the whole range of frequencies in which analysis was performed. The picture highlights that below 100 Hz measurements are noisy. Moreover, as highlighted by Garlando et al. (2021), stem electrical impedance varies over time in response to environmental parameter variations. These variations are less marked in the high-frequency range. Therefore, 1 kHz to 10 kHz is a more suitable range for analysis. From now on, a specific frequency is selected. Impedance analysis was carried out for a period of up one month.

Analyses highlighted that environmental conditions may be optimal even if the plant is suffering. In fact, figure 5 shows both impedance analysis and environmental sensors data collected in a period where the plant dries. Although data collected by environmental sensors do not show any drastic change, Figure 5 shows the characteristic behavior that the stem impedance has when a plant is about to dry completely. Impedance modulus has, at first, a significant drop, and then it boosts sharply. In fact, after this steep increase, $|Z|$ is around $5\text{ M}\Omega$, so at least two orders of magnitude greater than before. Plots showing the impedance after *Jan. 7th* are not reported since they are so higher than the previous one that it is impossible to find a suitable scale to show them clearly. In Figure 6 a picture taken on *Jan. the 7th* of the same plant analyzed in figure 5 is shown. It is easily noticeable that it is completely dried. Figure 5 shows that environment parameters had not underwent any dramatic change. Thus, exclusively monitoring environment parameters may not be enough to understand plant's health status.

Our work dealt with the first steps toward understanding a plant's health status through its stem impedance analysis. As a first step, it was important to find the relation between impedance and environmental condition, trying to understand how the impedance changes in reaction to the other parameters. Moreover, it was expected that every plant not to react in the same way in terms of absolute values. Thus a relative and statistical approach is by sure needed.

Impedance measurement was carried out once per hour, and it was performed together with the evaluation of data collected by the environment sensor. As stated previously, soil moisture sensor is reliable only

Plant2, Experiment 28 December - 08 January
Impedance measurement, stimulus signal frequency: 10145 Hz

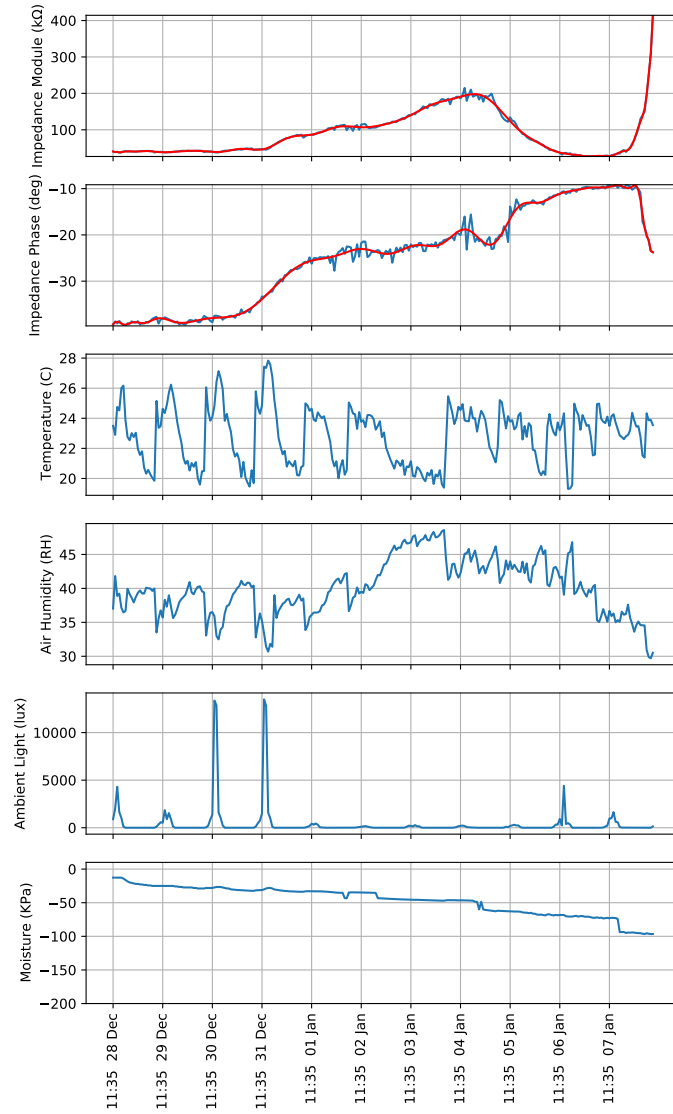


Figure 5: Plant stem's impedance modulus and phase presented with environment sensors data. These data have been collected right before the plant dies (see Figure 6). Red lines in the first two plots are 49th degree polynomial fitting curves of impedance modulus and phase.



Figure 6: Picture taken with a camera depicting the critical condition of the plant despite optimal environmental conditions (see Figure 5).

Plant1, Experiment 28 October - 28 November
Impedance measurement, stimulus signal frequency: 10145 Hz

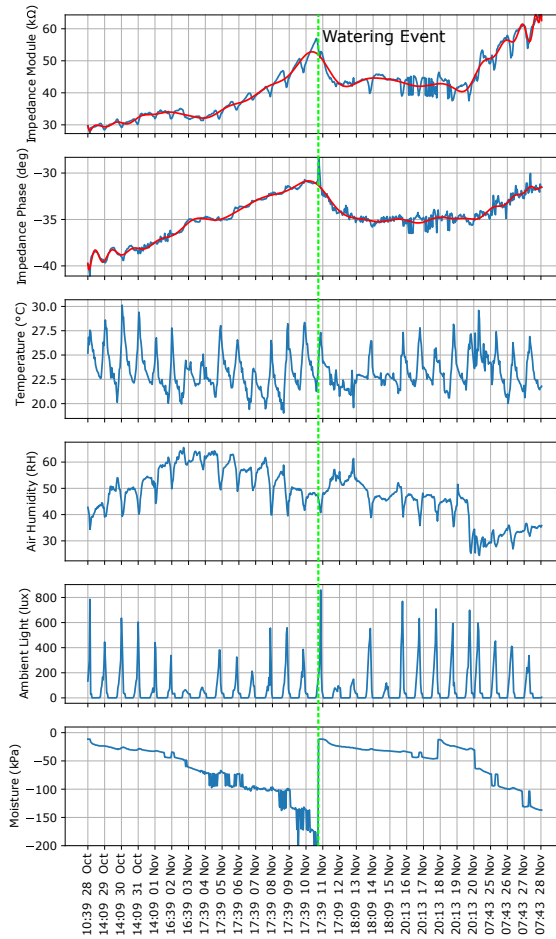


Figure 7: Stem impedance phase and modulus, ambient light, soil moisture, and air humidity evaluated for plant 1 between Oct. 28th and Nov. 28th. Red curves in the first two plots (modulus and phase) are 49th degree polynomial fitting curves, while the dashed vertical green line indicates the occurrence of a watering event.

231 down to -200 kPa. Thus, lower values were discarded and not reported in any of the plots.
232 Ambient light, temperature, and relative humidity were also reported in the figure. The experiment was per-
233 formed inside a laboratory. Therefore temperature is always above 20 °C. Figure 5 shows a clear relationship
234 between temperature and relative humidity. In Figure 7 data collected on plant 1 during the period *Oct. 28th*
235 to *Nov. 28th* are reported.

236 At the beginning of the considered period, a watering event occurred. Soil moisture value was approxi-
237 mately equal to 0 kPa, so water concentration inside the soil was maximum. While soil moisture level was de-
238 creasing, both impedance modulus and phase increased their value. After the watering event (dashed green
239 line in the figure), both modulus and phase presented a sharp drop followed by a period of stability. Phase
240 and modulus started to increase again when soil moisture level crossed the value of approximately -50 kPa.
241 This behavior suggested that there was a sort of cause-effect ratio linking soil moisture and impedance phase
242 and modulus. In fact, fitting curves shown in Figures 7, 8, and 9 have a flexion in correspondence of every
243 watering event. It is easily noticeable that, before every dashed green line, they increase and, after, decrease.
244 This behavior is repeatedly noticeable in Figure 9 where two watering events occurred. The first one was per-
245 formed when the soil was not completely dry, causing a modulus and phase drop less steep than the second
246 one.

247 Plant stem impedance modulus and phase show ripples both in their increasing and decreasing slopes.
248 Ripples repeat daily. It can be noticed that they appear when ambient light shows its peaks, thus when the
249 plant gets illuminated by the sun. This behavior suggested that the amount of light impinging on the plant
250 affects stem impedance. However, light, temperature, and humidity show very similar trends, and it is not
251 clear which is the reason behind daily impedance changes. Further analysis of ratios linking these quantities
252 will be carried out in the following section, where correlation and causality relations will be evaluated. Re-
253 sults reported in Figure 7 were not recorded for one plant only. Figures 8, and 9 demonstrate that similar
254 conclusions can be done for all plants and for different periods of time.

255 In particular, Figure 8 shows data of a different plant over twenty days. Soil moisture's curve shows

Plant2, Experiment 05 December - 25 December
 Impedance measurement, stimulus signal frequency: 10145 Hz

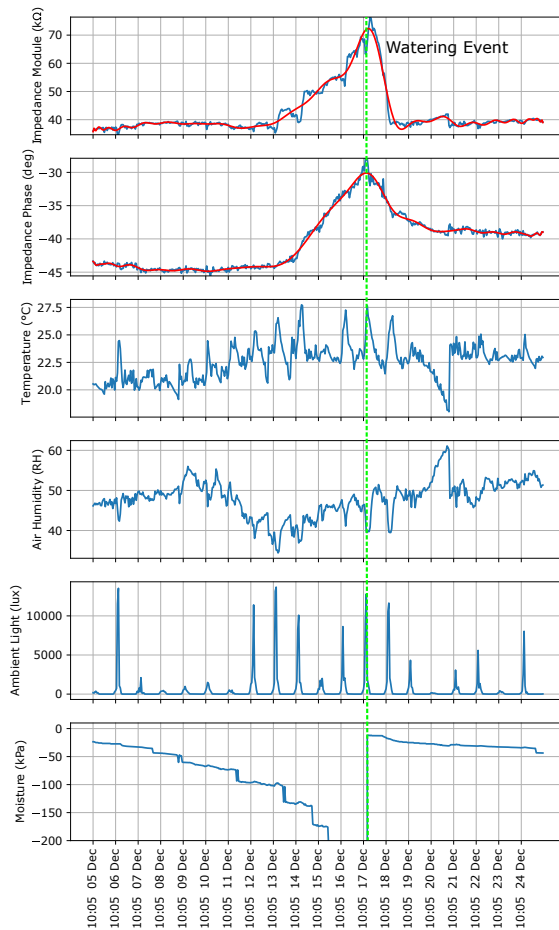


Figure 8: Impedance modulus and phase, and environment data collected during the period Dec. 5th to Dec. 25th for plant 2. Every impedance analysis was carried out at the frequency of 10 kHz. Soil moisture values lower than -200 kPa should not be considered and therefore not shown here. Red curves in the first two plots (modulus and phase) are 49th degree polynomial fitting curves, while the dashed vertical green line indicates the occurrence of a watering event.

Plant3, Experiment 31 October - 15 November
 Impedance measurement, stimulus signal frequency: 10145 Hz

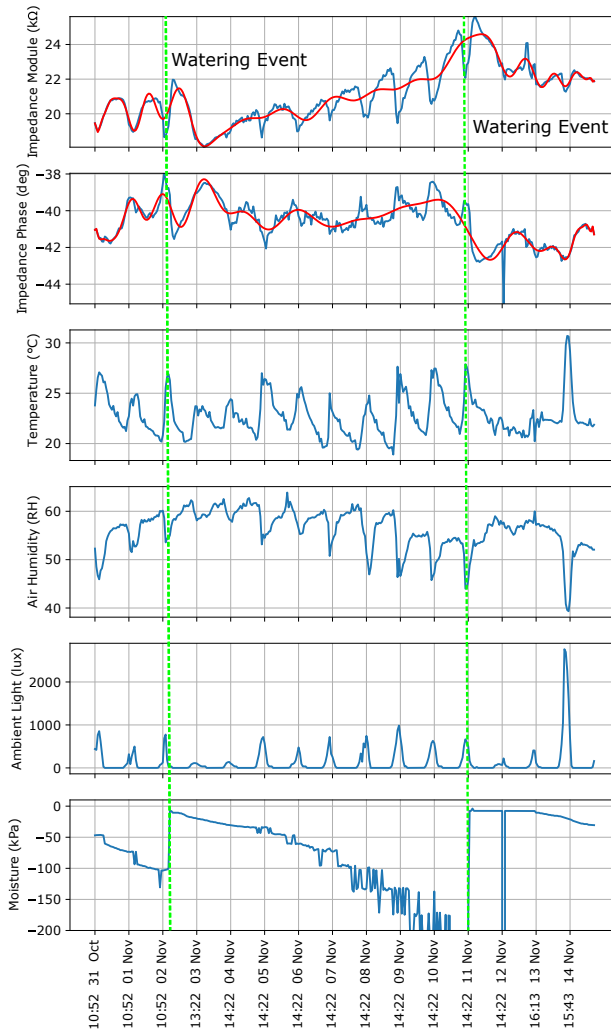


Figure 9: Impedance modulus and phase, and environment data collected during the period Oct. 31th to Nov. 15th for plant 3. Every impedance analysis was carried out at the frequency of 10 kHz. Soil moisture values lower than -200 kPa should not be considered and therefore not shown here. Red curves in the first two plots (modulus and phase) are 49th degree polynomial fitting curves, while the dashed vertical green lines indicate the occurrence of watering events.

256 that the plant was not watered until December, the 18th. Both impedance modulus and phase show similar
257 behavior as in the previous case. However, in this case, daily ripples are less marked. Figure 9 on the
258 contrary, shows clearly daily variations, but the trend due to soil drying is less evident.

259 Graphs reported in Figures 7,8, and 9 seem to indicate that soil moisture plays the most important role in
260 determining stem impedance modulus and phase trend. In fact, after watering events, they rapidly decrease.
261 Therefore, two more plants were tested to confirm our hypotheses. One of them (plant 5) was watered
262 frequently (twice per week) to keep its soil moisture level high and (almost) constant. The second one (plant
263 4) was subjected to water stress and watered exclusively when the soil was dry. Analysis was carried out
264 exactly in the same period of April 2021 for both of them. As stated in section 2.3, they were kept in the
265 same room and close to each other to have similar environmental conditions. In Figures 10 and 11 stems
266 impedance and environment data are reported. As expected, Figure 10 shows that stem impedance modulus
267 overall behavior increased before the watering event, while it steeply decreased afterward, showing the same
268 behavior seen in Figures 7, 8, and 9. In contrast, stem impedance reported in Figure 11 does not show a
269 clear overall trend. Impedance's changes are only due to the already mentioned daily ripples, and they are
270 milder than plant 4's ones. Same conclusions could not be drawn for stems impedance phase. In fact, in
271 Figure 10, it rises after the watering event. Thus, it is in contrast with the trend shown in Figures 7, 8, and 9.

272 To better understand how stem electrical impedance is affected by variations in the environment surround-
273 ing the plant, statistical tests exploited by Garlando et al. (2020b) were performed on both data coming from
274 environment sensors and impedance analyses. At first, the correlation matrix was computed to understand
275 how quantities are correlated with each other. Each matrix row and column is associated with a physical
276 quantity, and each value indicates the correlation between the two corresponding quantities; matrices are
277 symmetrical. Correlation values are adimensional real numbers in the range $[-1, 1]$ where -1 corresponds
278 to the highest level of anticorrelation and $+1$ to the highest correlation; if (nearly) 0, then the two quanti-
279 ties are not (significantly) related. A positive correlation implies that, statistically, two quantities increase (or
280 decrease) simultaneously. A negative one implies that they, statistically, have opposite behavior. Therefore

Plant 4 , Experiment 05 April - 21 April
 Impedance measurement, stimulus signal frequency: 10145 Hz

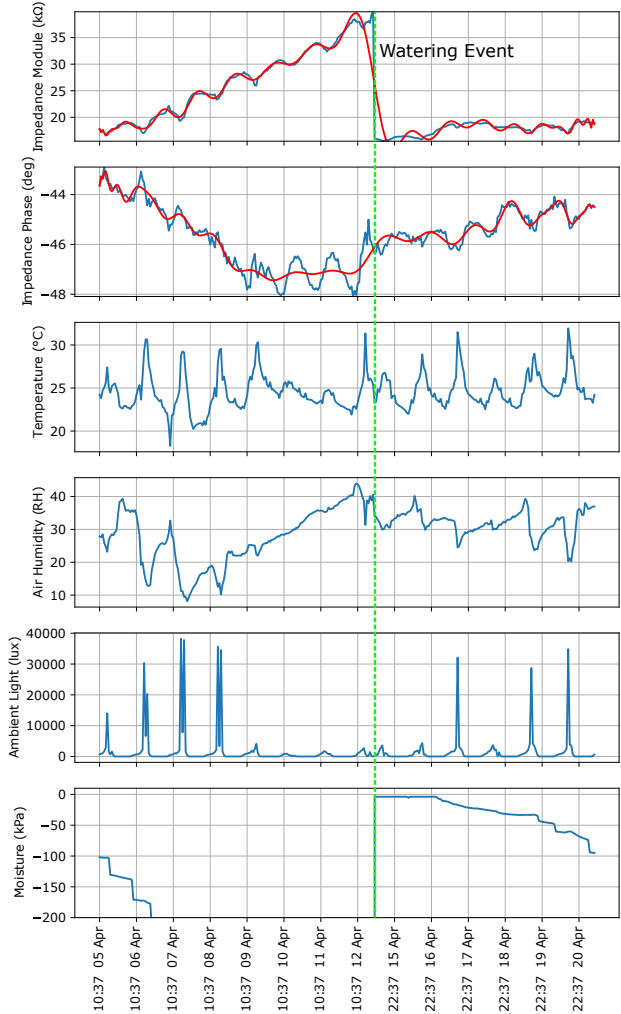


Figure 10: Impedance modulus and phase, and environment data collected during the period Apr. 5th to Apr. 21st for plant 4. Every impedance analysis was carried out at the frequency of 10 kHz. Soil moisture values lower than -200 kPa should not be considered and therefore not shown here. Red curves in the first two plots (modulus and phase) are 49th degree polynomial fitting curves, while the dashed vertical green lines indicate the occurrence of a watering events.

Plant 5 , Experiment 05 April - 21 April
Impedance measurement, stimulus signal frequency: 10145 Hz

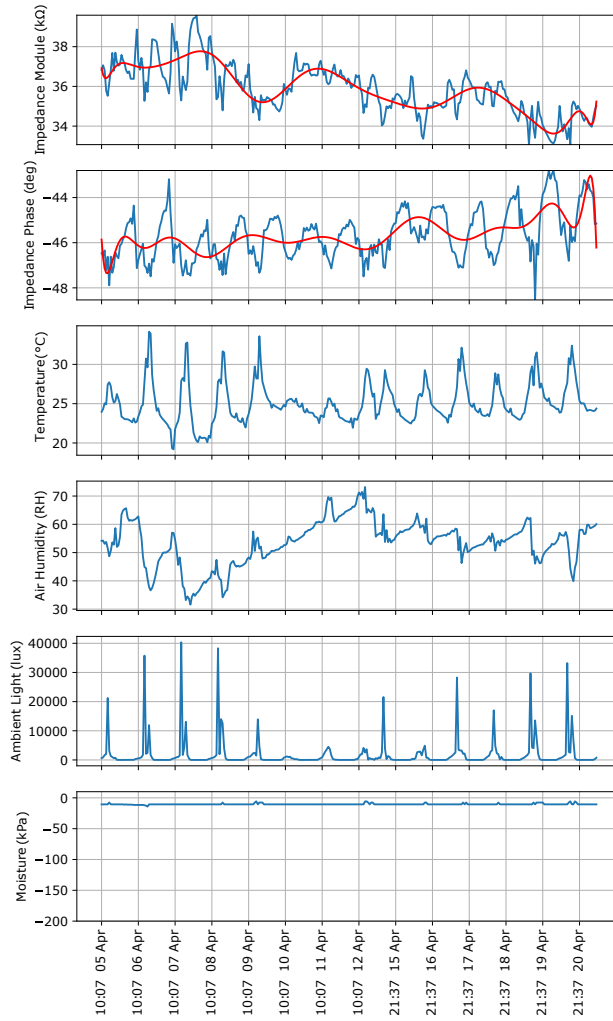


Figure 11: Impedance modulus and phase, and environment data collected during the period Apr. 5th to Apr. 21st for plant 5. Every impedance analysis has been carried out at the frequency of 10 kHz. Red curves in the first two plots (modulus and phase) are 49th degree polynomial fitting curves.

281 when one rises the other decreases and viceversa. Unfortunately, correlation does not imply causality. Thus,
282 to verify if a cause-effect ratio exists between two quantities, *Granger's* causality tests (Granger (1969)) were
283 performed, and related matrices were evaluated. This test indicates how valuable data relative to one of the
284 two quantities are to foresee the other's following values. If the test is successful, it is said that a quantity
285 "*Granger causes*" the other one. Data must be stationary to perform these statistical tests. Therefore, each
286 set of data (time series) used for the analysis underwent a stationary test. The first difference was applied
287 if it was not stationary, with each sample substituted by the difference with the previous one. The resulting
288 data were then tested again to avoid misleading results. Another essential parameter to be considered is the
289 lag parameter. It represents how many of the previous samples of one series are used to predict the new
290 values of the tested one. In this preliminary analysis, different lag values, ranging from one to eight, were
291 tested, the value resulting in the minimum matrix coefficient selected. In particular, in the results presented
292 here, a lag value equal to four was always chosen. Analyzed quantities are associated with rows and columns
293 of *Granger's* matrices, and the corresponding element indicates how significant the data for one quantity is
294 in predicting another one. A quantity is said to *Granger cause* the other one, with a 95% of confidence, if
295 the related matrix's element is lower than 0.05. If it is higher than the threshold, the test fails. The matrices
296 are not symmetrical: if a cause-effect relation holds, column quantity causes variations in the row's one, not
297 vice-versa. Figures showing correlation and *Granger's* matrices relative to plants 1,2, and 3 are reported in
298 the *Supplementary Material*.

299 Since this work aims to understand how the environment affects plant impedance behavior, the attention
300 will be focused on the correlation between stem impedance and environmental parameters. As expected, in
301 each correlation matrix, soil moisture is negatively correlated to stem impedance modulus. Water and sap's
302 flows inside the stem highly impact the impedance: under water stress, there is a flow reduction in the stem,
303 causing impedance modulus to increase.

304 Impedance phase, on the contrary, showed different behavior in experiments. It is highly correlated
305 with impedance modulus, but there is a positive correlation in some cases (plants 1 and 2) and negative in

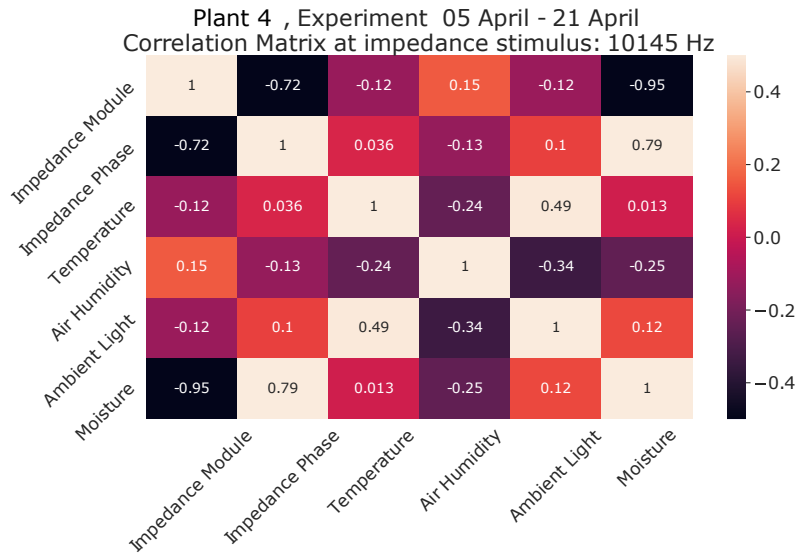


Figure 12: Correlation matrix evaluated for environmental and impedance data of plant 4 taken during the period 5/4/2021-21/4/2021.

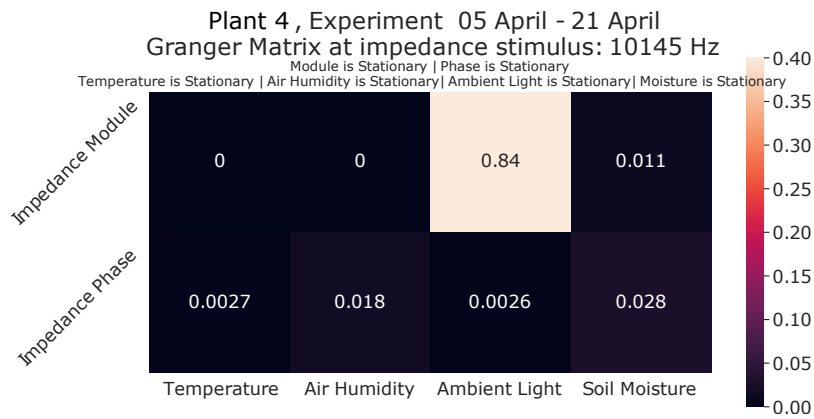


Figure 13: Granger's matrix evaluated for environmental and impedance data of plant 4 taken during the period 5/4/2021-21/4/2021.

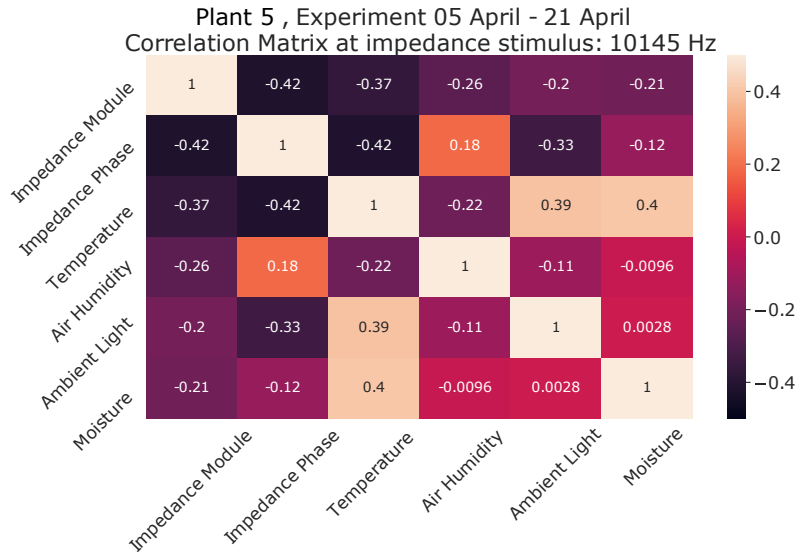


Figure 14: Correlation matrix evaluated for environmental and impedance data of plant 5 taken during the period 5/4/2021-21/4/2021.

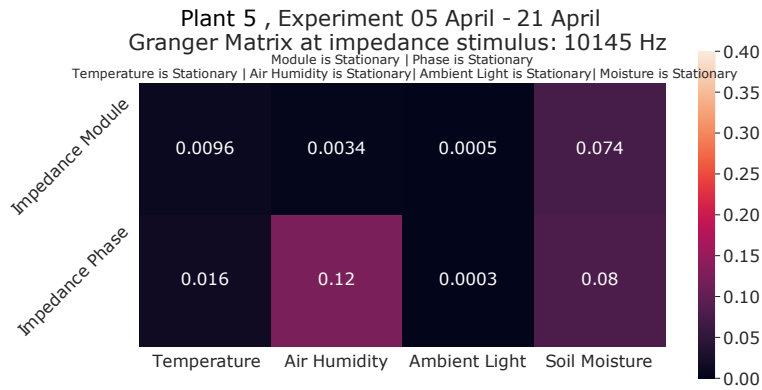


Figure 15: Granger's matrix evaluated for environmental and impedance data of plant 5 taken during the period 5/4/2021-21/4/2021.

306 others (plants 3, 4, and 5). Therefore, correlation between impedance and soil moisture was not common
307 among all the plants involved in the tests. Correlation between impedance and environmental parameters
308 was different in every experiment. Furthermore, the laboratory where experiments took place was not a
309 controlled environment: sunlight entering from windows caused an increase in temperature and a drop in
310 ambient humidity. This relation is visible in the correlation matrices, where values relative to these quantities
311 are similar in all experiments. However, the impact of temperature, light, and humidity is visible in the daily
312 trend of impedance modulus and phase (Garlando et al. 2021).

313 As mentioned before, *Granger's* causality test was performed on every data set. Matrices relative to
314 plant 1,2, and 3 are reported in the *Supplementary Material*. This analysis showed inconsistent results. For
315 example, plant 1 showed that all parameters, except soil moisture, are causing impedance modulus, while
316 all environmental parameters affect the impedance phase. Differently, from plant 2, it seems that all values
317 are causing both impedance modulus and phase. Thus, it is impossible to prove a causality relation among
318 different quantities valid for all plants and experiments. For this reason, the experiment involving plants 4
319 and 5 was performed to better understand how soil moisture affects stem electrical impedance. As already
320 mentioned, plant 5 was watered regularly, and it was analyzed together with plant 4 (subject to water stress),
321 used as a counter-check. As it can be seen in Figures 10 and 11, data acquired from environment sensors
322 are very similar. Only the air humidity show the same trend but in a different range: this may be due to more
323 intense evaporation, since soil moisture of plant 5 was overall significantly higher and kept almost constant.

324 Correlation between measured environmental parameters (plant 4 and 5) are reported in Table 1: with the
325 exception of ambient light whose sensor is significantly sensitive to its positioning with respect to the specific
326 plant, correlation values are nearly two order of magnitude greater than the soil moisture one. These results
327 confirm that the only significant difference between the environmental conditions of plant 4 and 5 is the soil
328 moisture.

329 Focusing on the correlation between electrical impedance and environmental conditions, and in particular,
330 on the first column of Figures 12 and 14, it is clear that in plant 5 impedance modulus is much less related

Table 1: Plant 4 and 5 environmental parameters correlation coefficients

	<i>Ambient Light</i>	<i>Air Humidity</i>	<i>Temperature</i>	<i>Soil Moisture</i>
<i>Correlation</i>	0,25	0,95	0,93	-0,016

Each value represents the correlation of the same quantity relative to the two plants.

331 to the soil moisture with respect to what happened for plant 4. The correlation coefficient equals -0.97 (very
 332 strong negative correlation) for plant 4, while it is -0.21 for plant 5 (mild anticorrelation). Conversely, the other
 333 environment parameters (temperature, air humidity, and ambient light) show a stronger correlation with stem
 334 impedance in plant 5. The comparison of impedance modulus variations between plants 4 and 5 and the
 335 experimental setup (plant 5 regularly watered and plant 4 subject to water stress) and correlation matrices
 336 results further reinforced the hypothesis that soil moisture can mostly affect stem impedance. As expected
 337 *Granger's* matrices for plant 4 and 5 (Figures 13 and 15) show that for the latter soil moisture is no more
 338 useful to foresee stem impedance values since, for plant 5, the coefficient is higher than 0.05. It leads to the
 339 conclusion that relevant changes in soil moisture cause significant changes in the stem impedance. However,
 340 otherwise, all the other environmental factors should be taken into account more thoroughly.

341 **4 Conclusion**

342 In this paper, a new sensor node to monitor different environmental parameters was presented. The node
 343 is small, cheap and exploits wireless communication. Given its properties, it was possible to use a node for
 344 each plant, placed directly close to it. Multiple nodes were used in a wireless sensor network to automatically
 345 monitor the environment, and a remote PC was used to collect all the data. Furthermore, a multiplexing
 346 circuit was used to measure the impedance of up to four plants simultaneously. This system was used to
 347 perform experiments to demonstrate the relations among impedance modulus, phase and plant status. The

348 relation between environmental conditions and plant status was derived from electrical impedance variations.
349 Various examples of water stress conditions were presented, together with the effects of temperature and light
350 intensity on impedance spectra. Furthermore, statistical analysis was performed on data acquired during
351 experiments: correlation among the different quantities is described, showing promising results. Indeed
352 correlation values as high as 95% were found among impedance and soil moisture. However, since correlation
353 does not imply causality, the "Granger causality" was tested. These analyses proved that soil moisture
354 statistically caused variations in the impedance of the plants. Nevertheless, soil moisture seems to be the
355 parameter that most affected both phase and modulus trends as shown in graphs 7, 8, 10 which show
356 environmental parameter data together with stem impedance. For these reasons, further analyses carried
357 out in controlled environments are needed to disentangle each environmental parameter's contribution to
358 stem impedance behavior over time. Moreover, since the amount of collected data will continue to grow,
359 machine learning algorithms will be implemented to better interpret them. This goal will be pursued in future
360 works.

361 **Funding** This research did not receive any specific grant from funding agencies in the public, commercial,
362 or not-for-profit sectors.

363 **References**

- 364 Bar-on, L., Jog, A., and Shacham-Diamand, Y. (2019a). "Four Point Probe Electrical Spectroscopy
365 Based System for Plant Monitoring". In: *2019 IEEE International Symposium on Circuits and
366 Systems (ISCAS)*, 1–5. URL: <https://ieeexplore.ieee.org/document/8702623>.
- 367 Bar-on, L. et al. (2019b). "In-Vivo Monitoring for Electrical Expression of Plant Living Parameters by
368 an Impedance Lab System". In: *2019 IEEE International Conference on Electronics, Circuits,
369 and Systems (ICECS)*. In press. URL: <https://ieeexplore.ieee.org/document/8964804>.

370 Bar-On, Lee et al. (2021). "Electrical Modelling of In-Vivo Impedance Spectroscopy of *Nicotiana*
371 *tabacum* Plants". In: *Frontiers in Electronics* 2, 14. URL: [https://www.frontiersin.org/
372 article/10.3389/felec.2021.753145](https://www.frontiersin.org/article/10.3389/felec.2021.753145).

373 Berenstein, Ron and Edan, Yael (2017). "Human-robot collaborative site-specific sprayer". In: *Jour-*
374 *nal of Field Robotics* 34.8, 1519–1530. URL: [https://onlinelibrary.wiley.com/doi/abs/
375 10.1002/rob.21730](https://onlinelibrary.wiley.com/doi/abs/10.1002/rob.21730).

376 Borges, E. et al. (2012). "Early detection and monitoring of plant diseases by Bioelectric Impedance
377 Spectroscopy". In: *2012 IEEE 2nd Portuguese Meeting in Bioengineering (ENBENG)*, 1–4.
378 URL: <https://ieeexplore.ieee.org/document/6331377>.

379 Burrell, A. L., Evans, J. P., and De Kauwe, M. G. (2020). "Anthropogenic climate change has driven
380 over 5 million km² of drylands towards desertification." In: *Nature Communications* 11 (1). URL:
381 <https://doi.org/10.1038/s41467-020-17710-7>.

382 Corono-Lopes, Diego D.J., Sommer, Sarah, Rolfe, Stephen A., Podd, Frank, and Grieve, Bruce
383 D. (2019). "Electrical impedance tomography as a tool for phenotyping plant roots". In: *Plant*
384 *Methods* 15. URL: <https://doi.org/10.1186/s13007-019-0438-4>.

385 Daskalakis, S. N., Assimonis, S. D., Kampianakis, E., and Bletsas, A. (2014). "Soil moisture wire-
386 less sensing with analog scatter radio, low power, ultra-low cost and extended communica-
387 tion ranges". In: *SENSORS, 2014 IEEE*, 122–125. URL: [https://ieeexplore.ieee.org/
388 document/6984948](https://ieeexplore.ieee.org/document/6984948).

389 European Environment Agency (2020). "Soil degradation - Environment in EU at the turn of the
390 century (Chapter 3.6)". In: Available Online (Last Modified 23 Nov 2020). URL: [https://www.
391 eea.europa.eu/publications/92-9157-202-0/page306.html](https://www.eea.europa.eu/publications/92-9157-202-0/page306.html).

- 392 Garlando, U., Bar-On, L., Avni, A., Shacham-Diamand, Y., and Demarchi, D. (2020a). “Plants and
393 Environmental Sensors for Smart Agriculture, an Overview”. In: *2020 IEEE SENSORS*, 1–4.
394 URL: <https://ieeexplore.ieee.org/document/9278748>.
- 395 Garlando, U. et al. (2020b). “Towards Optimal Green Plant Irrigation: Watering and Body Electrical
396 Impedance”. In: *2020 IEEE International Symposium on Circuits and Systems (ISCAS)*, 1–5.
397 URL: <https://ieeexplore.ieee.org/document/9181290>.
- 398 Garlando, Umberto et al. (2021). “Analysis of In Vivo Plant Stem Impedance Variations in Relation
399 with External Conditions Daily Cycle”. In: *2021 IEEE International Symposium on Circuits and
400 Systems (ISCAS)*, 1–5. URL: <https://ieeexplore.ieee.org/document/9401242>.
- 401 Granger, C. W. J. (1969). “Investigating Causal Relations by Econometric Models and Cross-
402 spectral Methods”. In: *Econometrica* 37.3, 424–438. URL: [http://www.jstor.org/stable/
403 1912791](http://www.jstor.org/stable/1912791).
- 404 Janesch, Jerry (2013). “Two-Wire vs. Four-Wire Resistance Measurements: Which Configuration
405 Makes Sense for Your Application?” In: *Keithley Instruments, Inc.*
- 406 Jinyang, Li, Meiqing, Li, Hanping, Mao, and Wenjing, Zhu (2016). “Diagnosis of potassium nu-
407 trition level in *Solanum lycopersicum* based on electrical impedance”. In: *Biosystems Engi-
408 neering* 147, 130–138. URL: [https://www.sciencedirect.com/science/article/pii/
409 S1537511016300666](https://www.sciencedirect.com/science/article/pii/S1537511016300666).
- 410 Kasama, T. et al. (2019). “Low Cost and Robust Field-Deployable Environmental Sensor for Smart
411 Agriculture”. In: *2019 2nd International Symposium on Devices, Circuits and Systems (ISDCS)*,
412 1–4. URL: <https://ieeexplore.ieee.org/document/8719262>.

413 Kobata, Kenji and Honda, Satoshi (2014). "Evaluating plant growth by utilizing Electrical Impedance
414 Analysis". In: *2014 Proceedings of the SICE Annual Conference (SICE)*, 113–118. URL: <https://ieeexplore.ieee.org/document/6935184>.
415

416 Mahato, Anupama (2014). "Climate change and its impact on agriculture". In: *International Journal
417 of Scientific and Research Publications* 4.4, 1–6.

418 Motto Ros, Paolo, Macrelli, Enrico, Sanginario, Alessandro, Shacham-Diamand, Yosi, and De-
419 marchi, Danilo (2019). "Electronic System for Signal Transmission Inside Green Plant Body".
420 In: *2019 IEEE International Symposium on Circuits and Systems (ISCAS)*, 1–5. URL: <https://ieeexplore.ieee.org/document/8702577>.
421

422 Nakayama, C., Katumata, T., Aizawa, H., Komuro, S., and Arima, H. (2008). "Two dimensional
423 evaluation of soil property for agriculture". In: *2008 International Conference on Smart Manu-
424 facturing Application*, 142–145. URL: <https://ieeexplore.ieee.org/document/4505629>.

425 Palazzi, V. et al. (2019). "Leaf-Compatible Autonomous RFID-Based Wireless Temperature Sen-
426 sors for Precision Agriculture". In: *2019 IEEE Topical Conference on Wireless Sensors and
427 Sensor Networks (WiSNet)*, 1–4. URL: <https://ieeexplore.ieee.org/document/8711808>.

428 Ramos-Giraldo, P. et al. (2020). "Low-cost Smart Camera System for Water Stress Detection in
429 Crops". In: *2020 IEEE SENSORS*, 1–4. URL: [https://ieeexplore.ieee.org/document/
430 9278744](https://ieeexplore.ieee.org/document/9278744).

431 Tenzin, S., Siyang, S., Pobkrut, T., and Kerdcharoen, T. (2017). "Low cost weather station for
432 climate-smart agriculture". In: *2017 9th International Conference on Knowledge and Smart
433 Technology (KST)*, 172–177. URL: <https://ieeexplore.ieee.org/document/7886085>.

434 UN. Population Division (2019). "World population prospects : 2019 : highlights". In: Available on-
435 line (viewed 30 July 2019)., 39 p. : URL: <http://digitallibrary.un.org/record/3813698>.